Available online at www.sciencedirect.com
ScienceDirect
Polymer 48 (2007) 6955–6964
polymer
www.elsevier.com/locate/polymer

On the structural and electronic properties of poly(3-thiophen-3-yl-acrylic acid methyl ester)

Oscar Bertran [a,*], Peter Pfeiffer [b], Juan Torras [a], Elaine Armelin [b], Francesc Estrany [c], Carlos Alemán [b,*]

[a] Departament d'Enginyeria Química, EUETII, Universitat Politècnica de Catalunya, Pça Rei 15, Igualada 08700, Spain
[b] Departament d'Enginyeria Química, E.T.S. d'Enginyers Industrials de Barcelona, Universitat Politècnica de Catalunya, Diagonal 647, Barcelona E-08028, Spain
[c] Unitat de Química Industrial, EUETIB, Universitat Politècnica de Catalunya, Comte d'Urgell 187, 08036 Barcelona, Spain

Received 16 July 2007; received in revised form 14 September 2007; accepted 17 September 2007

Abstract

Quantum chemical calculations on small idealized systems of poly(3-thiophen-3-yl-acrylic acid methyl ester), a new polythiophene derivative soluble in polar solvents, have been performed to propose a model for this polymer. The model, which was derived from calculations at the HF/6-31G(d) and B3PW91/6-31+G(d,p) levels is defined by both the head-to-tail polymer linkages and the conformation of the acrylic acid methyl ester side groups. The $\pi-\pi^*$ lowest transition energy predicted for the polymer is in excellent agreement with the experimental values, which were determined in this work using UV–visible experiments. Finally, we investigated the variation of the electronic properties produced by small chemical modifications in the side group of poly(3-thiophen-3-yl-acrylic acid methyl ester), such changes being designed to enhance the solubility of the polymer in water.

Keywords: Polythiophene; Transition energy; Computer modeling

1. Introduction

Among organic semiconducting polymers, polythiophene derivatives have been the subject of intense study due to their many interesting electronic and optical properties [1–3]. The main drawback of many of these polymers is their lack of solubility, which explains their limited processability. A partial solution to this problem has been the insertion of suitable substituents: introduction of long alkyl side chains increases the solubility in organic solvents [4–8], whereas hydrophilic substituents produce water-soluble polythiophenes [9–16].

At present we are particularly interested in polymers able to solubilize in polar solvents, especially in polythiophenes containing electron-withdrawing alkyl carboxylate substituents. In earlier studies in this field, Pomerantz and co-workers investigated the role of carboxylate groups on the structure of polythiophenes containing ester functionalities directly attached to the thiophene ring [17–20]. For this purpose, the structure of 2,2′-bithiophenes incorporating methyl carboxylate substituents at the 3,3′-, 3,4′- and 4,4′-positions was analyzed using X-ray diffraction. More recently, we investigated the conformational and electronic properties of these compounds using quantum mechanical methods [21]. The calculated properties were in agreement with those of both small oligomers [26–29] and poly(alkyl thiophene-3-carboxylates) [11] with a carbonyl group directly attached to the ring. Furthermore, we used theoretical calculations to predict changes in the interactions between the side chain functionality and the backbone when the alkyl group is removed, *i.e.* a carboxylic acid group is directly attached to the thiophene ring [22].

* Corresponding authors.
E-mail addresses: oscar@euetii.upc.edu (O. Bertran), carlos.aleman@upc.edu (C. Alemán).

0032-3861/$ - see front matter © 2007 Elsevier Ltd. All rights reserved.
doi:10.1016/j.polymer.2007.09.033

In this work, we apply quantum chemical methods to examine the structural and electronic properties of poly(3-thiophen-3-yl-acrylic acid methyl ester), hereafter denoted as PT3AME (Scheme 1), a new polythiophene derivative with a conjugated substituent in which the polymer backbone and the electron-withdrawing carboxylate group are separated by a double bond. The functionalizaton of polythiophene with an acrylate group was pursued in the past to promote crosslinking of the polymer chains for controlled hardening of polymers, or to functionalize the conducting backbone with a group amenable of further functionalizations [23–25]. However, in such acrylate-functionalized polythiophenes the orientation of the side chain was opposite to that in PT3AME, *i.e.* the polymer backbone and the double bond of the acrylate group were separated by the alkyl carboxylate moiety. It is worth noting that the aim of the acrylate substituent in PT3AME is not only to improve the solubility of polythiophene but also to enlarge the conjugated system from the backbone to the side chain. This is expected to improve the electronic properties with respect to unsubstituted polythiophene by reducing the values of the lowest transition energy (ε_g) and ionization potential (IP).

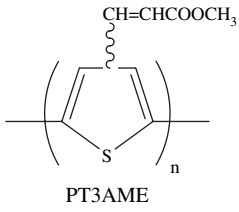

PT3AME

Scheme 1.

In this paper we use quantum mechanical calculations to propose an atomistic model study for PT3AME, experimental measures being also reported to confirm the reliability of our predictions. This model is based on an exhaustive conformational study on small systems containing one and two monomeric units. The ε_g, which is the most characteristic electronic property of conducting polymers, predicted for PT3AME using such model has been compared with experimental values. For this purpose UV–visible experiments in different environments were conducted on PT3AME, which was prepared and characterized within a wide project devoted to prepare soluble polythiophene derivatives by incorporating carboxylate-containing substituents of very different chemical nature [26]. The excellent agreement between the experimental and theoretical values allowed us to predict the ε_g of other related polythiophene derivatives. Thus, the influence on this important electronic property of small chemical modifications in the acrylic acid methyl ester (AME) substituent has been examined.

2. Methods

2.1. Computational methods

Full geometry optimizations of oligomers containing *n* monomeric units (*n*-T3AME) with *n* ranging from 1 to 6 were performed using the Hartree–Fock method combined with the 6-31G(d) basis set [27], *i.e.* HF/6-31G(d) level. Previous studies indicated that this simple methodology is able to provide a very satisfactory description of the molecular geometry and relative energy for the minimum energy conformations of heterocyclic oligomers like those studied in this work [28,29]. Calculations on 2-T3AME oligomers were carried out considering both the *anti-gauche* ($\theta = 150°$) and *syn-gauche* ($\theta = 30°$) conformations as starting structures, the inter-ring dihedral angle θ being defined by sequence S–C–C–S. Thus, previous studies on disubstituted 2,2′-bithiophene derivatives indicated that these conformations are relatively close to those typically identified as global and local minima, respectively [21,22,30].

The Koopmans' theorem [31] was used to estimate the ionization potentials (IPs). Accordingly, IPs were taken as the negative of the highest occupied molecular orbital (HOMO) energy, *i.e.* $IP = -\varepsilon_{HOMO}$. The IP indicates if a given acceptor (p-type dopant) is capable of ionizing, at least partially, the molecules of the compound. The $\pi-\pi^*$ lowest transition energy (ε_g) was approximated as the difference between the HOMO and lowest unoccupied molecular orbital (LUMO) energies, *i.e.* $\varepsilon_g = \varepsilon_{LUMO} - \varepsilon_{HOMO}$. Although HF calculations provide a satisfactory qualitative description of the electronic properties of polyheterocyclic molecules, we are aware that this method tends to overestimate the values of IP and ε_g [32,33]. Accordingly, the electronic properties presented in this work have been estimated performing single point Density Functional Theory (DFT) calculations with the B3PW91 method [34,35] combined with the 6-31G(d,p) basis set [36] (B3PW91/6-31G(d,p)) on the molecular geometries optimized at the HF/6-31G(d) level. It is worth noting that according to the Janak's theorem [37], the approximation mentioned above for the calculation of the IP can be applied to DFT calculations, while Levy and Nagy evidenced that ε_g can be rightly approximated as the difference between ε_{LUMO} and ε_{HOMO} in DFT calculations [38].

The electronic properties of PT3AME have been related with the degree of aromatic character. For this purpose, we examined the C–C bond length alternation pattern along the π-system of the backbone and, in particular, the inter-ring distances *d*. Furthermore, we evaluated the aromaticity of the cycles using the Julg parameter (JP) [39], a geometric criterion used to measure the deviations of the individual C–C bond lengths (r_i) from the mean C–C bond distance (r) in the diene unit of the cycles:

$$JP = 1 - \frac{225}{3}\sum_{i=1}^{3}\left(1 - \frac{r_i}{r}\right)^2 \quad (1)$$

2.2. Experimental methods

3-Thiophen-3-yl-acrylic acid (3TA) and anhydrous ferric chloride were purchased from Sigma-Aldrich Química S.A. and were employed without further purification. All solvents were purchased from Panreac Química S.A. with ACS grade.

FTIR spectra were recorded on a 4100 Jasco spectrophotometer equipped with an ATR MKII Golden Gate Heated Single Reflection Diamond Specac model. Proton NMR spectra were recorded on a Varian Inova 300 spectrometer operating at 300.1 MHz. The UV–visible optical spectra of the polymer were obtained from their 1 mg/mL solutions in acetone and DMSO using a Shimadzu UV-240 Graphtcord UV–visible recording spectrophotometer.

2.2.1. Monomer synthesis

3TA (3 g) was refluxed in dry methanol (15 mL) with one drop of concentrated sulfuric acid for 24 h to provide 3-thiophen-3-yl-acrylic acid methyl ester (T3AME). The purification of this monomer, which was obtained with 99.9% of yield, was carried out by the evaporation of methanol and successive extraction with diethyl ether. The extract was washed with distilled water, dried with anhydrous $MgSO_4$, and filtered washing several times with diethyl ether. The product was recovered after evaporation of the solvent.

2.2.2. Preparation of PT3AME

Polymerization of T3AME monomer was performed by chemical oxidative coupling in dry chloroform using anhydrous ferric chloride, according to the procedure described by Yoshino et al. [40] in 1989. A solution of 20 mmol of monomer in 40 mL of chloroform was added dropwise to a solution of 80 mmol of ferric chloride in 60 mL of dry chloroform. The mixture was stirred for 24 h and then stored in the freezer overnight. In order to precipitate PT3AME, the product was poured out into a large excess of methanol (2 L) and, subsequently, purified by repeated washing with methanol and distilled water. After removal of the residual $FeCl_3$, the polymer was dried under vacuum at 40 °C for 72 h.

3. Results and discussion

3.1. Modeling of the monomeric unit: intrinsic conformational preferences of the AME side group and its interactions with the thiophene ring

In order to ascertain the intrinsic conformational preferences of the AME substituent, calculations on a single monomeric unit were performed considering all the possible arrangements of this side group, *i.e.* those that are consequence of the *cis* ↔ *trans* isomerism around the dihedral angles associated with the AME group. The eight arrangements obtained after geometry optimization are displayed in Fig. 1. Inspection to the relative energies, which have been reported in the figure, indicates that conformations I–IV are significantly more stable than V–VIII. This is because the methyl carboxylate moiety interacts repulsively with the α-hydrogen atom of the thiophene ring in the latter four arrangements. Indeed, the strength of such interactions induces strong distortion from planarity in V and VII, *i.e.* in these two arrangements the methyl carboxylate and the aromatic ring are not located in the same plane. On the other hand, structures II–IV are destabilized with respect to I, which is the lowest energy minimum, by less than 2.5 kcal/mol. The most remarkable feature of I–IV is the absence of strong repulsive contacts between the thiophene ring and the side chain. It should be mentioned that the nomenclature used in Fig. 1 to denote each arrangement of the AME group, *i.e.* labels I-to-VIII, has been also used for 2-T3AME isomers and PT3AME throughout the whole work.

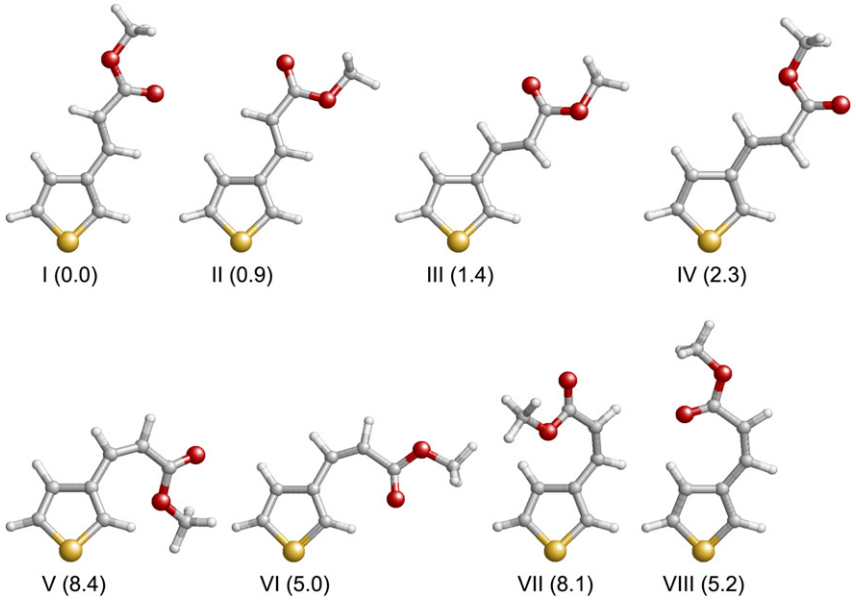

Fig. 1. Minimum energy conformations of 3-thiophen-3-yl-acrylic acid methyl ester (T3AME) calculated at the HF/6-31G(d) level. Relative energies (in kcal/mol) are displayed in parenthesis.

3.2. Modeling of the dimeric units: relative stability and conformational analysis of the three isomeric 2,2′-bithiophenes

Quantum chemical calculations have been used to examine the relative stability and conformational preferences, in terms not only of the side chain arrangement but also of the inter-ring dihedral angle θ, of three possible isomers of 2-T3AME. These compounds differ in the positions substituted by AME side groups: 4,4′ (2-T3AME$_{4,4'}$), 3,3′ (2-T3AME$_{3,3'}$) and 3,4′ (2-T3AME$_{3,4'}$). It should be noted that they should be considered as model systems of the tail-to-tail, head-to-head and head-to-tail polymer linkages, respectively. Thus, the regiochemistry of polymer chains is defined during the polymerization process, which takes place in solution. Therefore, the choice of the most probable polymer linkage mainly depends on the attractive or repulsive interactions between monomeric units directly bonded. This allows us to predict the regiochemistry of polymer chains using simple models containing two monomeric units, as those studied in this section, rather than complex models that involve large polymer chains and/or inter-molecular interactions.

As was evidenced in the previous subsection for 1-T3AME, the side groups of 2-T3AME may adopt many different arrangements, which are expected to affect not only the inter-ring dihedral angle but also the relative stability of the different isomers. In order to get a deeper insight into this dependence, we examined the minimum energy conformations of 2-T3AME$_{4,4'}$, 2-T3AME$_{3,3'}$ and 2-T3AME$_{3,4'}$ considering the eight orientations displayed in Fig. 1 for each AME side chain. Accordingly, the number of starting structures that were considered for the 2-T3AME$_{4,4'}$ and 2-T3AME$_{3,3'}$ isomers was:

$$\begin{aligned}&(2\ \text{minima for the internal rotation of}\ \theta:\\ &\quad anti-gauche\ \text{and}\ syn-gauche)\\ &\times\left(\left[8^2-\binom{8}{2}\right]\ \text{arrangements of the two side chains}\right)\\ &\quad =72\ \text{per compound.}\end{aligned}$$

For the 2-T3AME$_{3,4'}$ isomer, the number of starting structures increased to $2\times 8^2=144$ since in this case substitution at positions 3,4′ and 4,3′ are not identical. Complete geometry optimization at the HF/6-31G(d) level led to 72, 38 and 102 minimum energy conformations for 2-T3AME$_{4,4'}$, 2-T3AME$_{3,3'}$ and 2-T3AME$_{3,4'}$, respectively, *i.e.* 212 minima from an initial set of 272 structures.

The lowest energy conformation, which is displayed in Fig. 2a, corresponds to the 2-T3AME$_{4,4'}$ isomer. As expected, this structure corresponds to an *anti-gauche* conformation ($\theta=145.7°$) with the AME groups arranged like in the structure I of 1-T3AME. Furthermore, six local minima with a relative energy smaller than 2 kcal/mol were detected for the 2-T3AME$_{4,4'}$ isomer. Structural details of such local minima are given in Table 1, which also include the values of IP and ε_g predicted at the HF/6-31G(d) level. The first local minimum (Fig. 2b), 2#-4,4′, is destabilized by 0.6 kcal/mol. This structure is identical to the lowest energy one but with the inter-ring dihedral angle arranged in *syn-gauche* ($\theta=46.4°$). The other local minima listed in Table 1, with the exception of

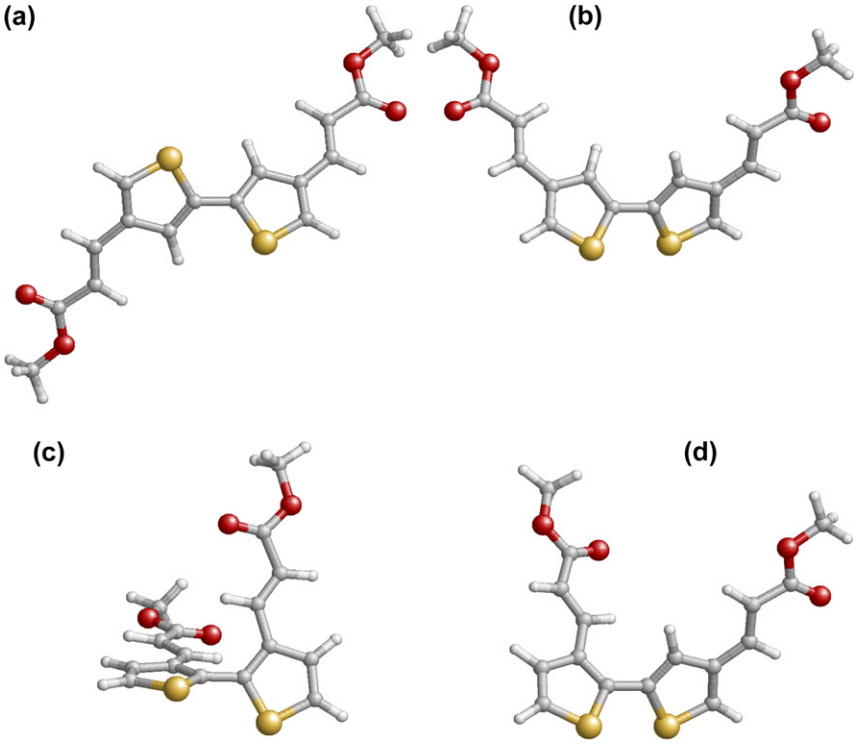

Fig. 2. Selected minimum energy conformations of the 2-T3AME isomers calculated at the HF/6-31G(d) level: (a) 1#-4,4′; (b) 2#-4,4′; (c) 1#-3,3′; and (d) 1#-3,4′. The structural characteristics of these minima are described in Tables 1–3.

Table 1
Structural and electronic properties of the minimum energy conformations of 2-T3AME$_{4,4'}$ with relative energy (ΔE, in kcal/mol) smaller than 2.0 kcal/mol (calculations were performed at the HF/6-31G(d) level)

Label	θ[a]	AME groups[b]	ΔE	IP[c]	ε_g[c]
1#-4,4′	145.9	I (4)/I (4′)	0.0	8.21	10.21
2#-4,4′	46.4	I (4)/I (4′)	0.6	8.32	10.38
3#-4,4′	146.0	II (4)/I (4′)	0.9	8.22	10.21
4#-4,4′	145.7	III (4)/I (4′)	1.4	8.18	10.05
5#-4,4′	46.1	II (4)/I (4′)	1.5	8.32	10.38
6#-4,4′	146.0	II (4)/II (4′)	1.9	8.22	10.22
7#-4,4′	45.8	III (4)/I (4′)	2.0	8.28	10.20

[a] Inter-ring dihedral angle in degrees.
[b] Arrangement of the acrylic acid methyl ester groups bonded to 4 and 4′. The arrangement of the side groups has been categorized according to Fig. 1.
[c] Ionization potential (IP) and π−π* lowest transition energy (ε_g) in eV.

5#-4,4′, differ in the conformation of the AME groups, the difference between the latter and 3#-3,3′ being the internal rotation θ.

A detailed inspection to the results displayed in Table 1 reveals that the energy contributions associated with the arrangement of the side group in each monomeric unit of 2-T3AME$_{4,4'}$ are related to the relative energies calculated for 1-T3AME (Fig. 1) that, in addition, are additive. For example, the relative energy of the minimum labelled 3#-4,4′ is 0.9 kcal/mol, which is exactly the relative energy found for the arrangement II is 1-T3AME (Fig. 1). The same behaviour is shown by all the local minima with two AME side chains displaying arrangements different from I. Specifically, the relative energy of 6#-4,4′ is 1.9 kcal/mol, which is very close to 2×0.9 kcal/mol. Fig. 3 represents the relative energy of all the minimum energy conformations found for 2-T3AME$_{4,4'}$ against θ. In the highest energy minimum with an *anti-gauche* conformation, which is destabilized by 16.6 kcal/mol, the two AME groups adopt the arrangement categorized as V in Fig. 1. As can be seen, the relative energy of this conformation is very close to 2×8.4 kcal/mol. These results clearly indicate that there is neither any interaction between the two side groups nor between a given side chain and the neighboring thiophene ring.

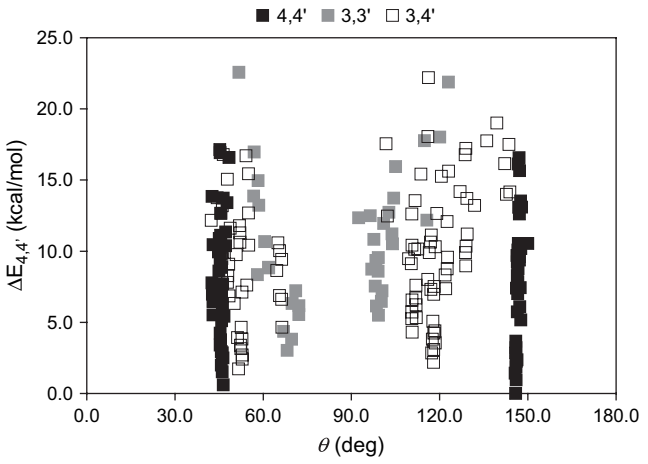

Fig. 3. Relative energy with respect to the lowest energy minimum of the most stable isomer ($\Delta E_{4,4'}$) of all the minimum energy conformations found for 2-T3AME$_{4,4'}$ (black squares), 2-T3AME$_{3,3'}$ (gray squares) and 2-T3AME$_{3,4'}$ (empty squares) against the inter-ring dihedral angle θ.

The lowest energy conformation found for the 2-T3AME$_{3,3'}$ isomer is displayed in Fig. 2c. In this structure, which is 3 kcal/mol less stable than the global minimum of 2-T3AME$_{4,4'}$, the two rings tend to adopt an almost perpendicular conformation ($\theta = 68.1°$) with the AME groups arranged as in I. Table 2 lists the structural and electronic characteristics of the three minima found for 2-T3AME$_{3,3'}$ within a relative energy range of 2 kcal/mol, the relative energy with respect to the lowest energy minimum of the most stable isomer ($\Delta E_{4,4'}$) being also displayed. Obviously, the conformational flexibility of the 2,2′-bithiophene derivatives is more restricted when the substituents are attached at positions 3,3′ than when they are at positions 4,4′. This is reflected by the reduced number of minima found for 2-T3AME$_{3,3'}$, which is due to the fact that the *anti-gauche* and *syn-gauche* minima found in 2-T3AME$_{4,4'}$ for each combination of AME arrangements usually transform into a single minimum with the two rings almost perpendicular in 2-T3AME$_{3,3'}$. Thus, the inter-ring dihedral angle θ is severely distorted with respect to the values found for the minima of 2-T3AME$_{4,4'}$. Fig. 3, which shows $\Delta E_{4,4'}$ against θ for all the minima of 2-T3AME$_{3,3'}$, evidences that θ is typically located at $\sim 70°$ or $\sim 100°$, these values being relatively close to that ideally expected for the *gauche−gauche* conformation ($\theta = 90°$). The distinctive conformational properties of 2-T3AME$_{3,3'}$ are consequence of the strong steric interactions between each AME side group and its neighbor thiophene ring, which are minimized when the two rings are arranged in an almost perpendicular conformation.

Regarding the 2-T3AME$_{3,4'}$ isomer, Table 3 lists the more relevant information of the eight minima found within a relative energy range of 2 kcal/mol. As can be deduced from the values of θ, the conformational characteristics of these structures are intermediate between those of the minima of 2-T3AME$_{4,4'}$ and 2-T3AME$_{3,3'}$. Comparison of the inter-ring dihedral angle of all the minima found for the three isomers (Fig. 3) also evidences this feature. Furthermore, it is worth noting that the stability of the 2-T3AME$_{3,4'}$ isomer is also

Table 2
Structural and electronic properties of the minimum energy conformations of 2-T3AME$_{3,3'}$ with relative energy (ΔE, in kcal/mol) smaller than 2.0 kcal/mol

Label	θ[a]	AME groups[b]	ΔE	$\Delta E_{4,4'}$	IP[c]	ε_g[c]
1#-3,3′	68.1	I (3)/I (3′)	0.0	3.0	8.43	10.30
2#-3,3′	69.7	II (3)/I (3′)	0.8	3.8	8.51	10.34
3#-3,3′	66.9	II (3)/II (3′)	1.3	4.4	8.53	10.28

The relative energy with respect to the lowest energy minimum of the most stable isomer (minimum 1-#4,4′) ($\Delta E_{4,4'}$, in kcal/mol) is also displayed. Calculations were performed at the HF/6-31G(d) level.
[a] Inter-ring dihedral angle in degrees.
[b] Arrangement of the acrylic acid methyl ester groups bonded to 3 and 3′. The arrangements of the side groups have been categorized according to Fig. 1.
[c] Ionization potential (IP) and π−π* lowest transition energy (ε_g) in eV.

Table 3
Structural and electronic properties of the minimum energy conformations of 2-T3AME$_{3,4'}$ with relative energy (ΔE, in kcal/mol) smaller than 2.0 kcal/mol

Label	θ[a]	AME groups[b]	ΔE	$\Delta E_{4,4'}$	IP[c]	ε_g[c]
1#-3,4′	51.7	I (3)/I (4′)	0.0	1.7	8.28	10.11
2#-3,4′	118.0	I (3)/I (4′)	0.5	2.2	8.34	10.30
3#-3,4′	52.8	II (3)/I (4′)	0.7	2.4	8.35	10.16
4#-3,4′	52.8	I (3)/II (4′)	1.0	2.7	8.29	10.14
5#-3,4′	117.3	II (3)/I (4′)	1.1	2.8	8.45	10.34
6#-3,4′	118.0	I (3)/II (4′)	1.4	3.1	8.39	10.31
7#-3,4′	52.4	II (3)/II (4′)	1.4	3.1	8.26	10.03
8#-3,4′	118.5	I (3)/III (4′)	1.8	3.5	8.34	10.24

The relative energy with respect to the lowest energy minimum of the most stable isomer (minimum 1-#4,4′) ($\Delta E_{4,4'}$, in kcal/mol) is also displayed. Calculations were performed at the HF/6-31G(d) level.

[a] Inter-ring dihedral angle in degrees.

[b] Arrangement of the acrylic acid methyl ester groups bonded to 3 and 4′. The arrangements of the side groups have been categorized according to Fig. 1.

[c] Ionization potential (IP) and π−π* lowest transition energy (ε_g) in eV.

intermediate between those of the 2-T3AME$_{4,4'}$ and 2-T3AME$_{3,3'}$ ones, *i.e.* the $\Delta E_{4,4'}$ value of the lowest energy minimum of 2-T3AME$_{3,4'}$ and 2-T3AME$_{3,3'}$ is 1.7 and 3.0 kcal/mol, respectively. On the other hand, the AME side groups of the lowest energy minimum of 2-T3AME$_{3,4'}$ adopt an I-like arrangement (Fig. 2d), which is fully consistent with the results obtained for 2-T3AME$_{4,4'}$ and 2-T3AME$_{3,3'}$.

Finally, inspection of the IP and ε_g values displayed in Tables 1−3 reveals that variations of both the molecular conformation and the chemical structure do not introduce significant changes in these electronic properties. Thus, the gaps predicted for the three isomers are very similar. However, it should be emphasized that these results should be considered from a qualitative point of view since it is well known that the HF method tends to overestimate significantly the values of IP and ε_g [29].

3.3. PT3AME: proposed model, calculation of the electronic properties and comparison with experimental data

As was discussed above, molecules constituted by two monomeric units should be considered as small model systems of polymer chains because they provide information about the linkages between consecutive units. In this section the results provided by the extensive conformational studies performed on 2-T3AME$_{4,4'}$, 2-T3AME$_{3,3'}$ and 2-T3AME$_{3,4'}$ have been used to develop an idealized model for infinite polymer chains of PT3AME, which will be used to predict its electronic properties.

Results displayed in Fig. 3 and Tables 1−3 indicate that AME side groups should be arranged as in I (see Fig. 1) and separated as much as possible. Fig. 4a represents the model proposed for PT3AME for an oligomer formed by six monomeric units. As can be seen, head-to-tail polymer linkages that are repeated along the chain constitute it. Thus, the $\Delta E_{4,4'}$ values obtained for 2-T3AME isomers indicate that this situation is more stable than that formed by alternating tail-to-tail and head-to-head polymer linkages. The reliability of this prediction was experimentally confirmed using NMR spectroscopy. Thus, splitting of the $-COOCH_3$ signal of PT3AME, which was prepared using the synthetic procedure described in Section 2, was used to provide information about the ratio of head-to-tail, head-to-head and tail-to-tail diads arising from polymerization. This was performed using the procedure previously reported for poly(3-dodecylthiophene) [41], which is based on an accurate analysis of the protons from 3.7−3.0 ppm region in the ^{1}H NMR spectra. Analyses of peak areas obtained in deuterated chloroform showed that the head-to-tail is the predominant linkage (∼80%), the remaining ones being of the head-to-head type.

According to the overall results, the head-to-tail model was used to build oligomers containing n monomeric units with $n = 2-6$ (Fig. 4a), which were completely optimized at the HF/6-31G(d) level. Additional calculations on selected oligomers ($n = 2$, 4 and 6) constructed by alternating tail-to-tail and head-to-head linkages (Fig. 4b) revealed that the stability of the head-to-tail model grows with the number of monomeric units confirming that the latter model is the most stable. This feature is reflected in Fig. 5a.

Previous studies [42,33] indicated that, in order to extrapolate the electronic properties calculated for oligomers to infinite chain polymers, conformational effects should be omitted by imposing an all-*anti* conformation (see below). Furthermore, it is well known that, in the solid state, molecular chains of heterocyclic conducting polymers and oligomers tend to adopt planar structures to optimize the packing interactions [41]. Accordingly, in order to predict the electronic properties of PT3AME, the molecular geometries of *n*-T3AME oligomers were re-optimized fixing the inter-ring dihedral angles θ at 180°. Fig. 5b, which compares the energies of the all-*anti* and fully optimized conformations for the *n*-T3AME oligomers constructed using the head-to-tail linkages, shows that the penalty imposed by the planarity to the proposed model is very low.

In order to evaluate the ε_g and IP, single point calculations at the B3PW91/6-31G(d,p) level were performed on the optimized geometries of oligomers containing head-to-tail linkages. Fig. 6 shows perfect linear behaviours (correlation coefficient $r > 0.99$) for the variation of the calculated ε_g and IP with the inverse chain length ($1/n$). A linear regression analysis, which is also displayed in Fig. 6, allowed extrapolate ε_g and IP values of 2.28 and 5.11 eV, respectively, for an infinite chain of PT3AME. It is worth noting that this extrapolation is not possible when the electronic properties of completely optimized oligomers are used since the relatively random disposition of *anti-gauche*$^+$ and *anti-gauche*$^-$ disturbs such linear behaviour. On the other hand, the ε_g and IP values estimated for the model constructed by alternating tail-to-tail and head-to-head linkages, were 2.51 and 5.36 eV, respectively. However, these values, which were derived considering selected oligomers ($n = 2$, 4 and 6), have not been considered for further discussion because of the low stability of the model.

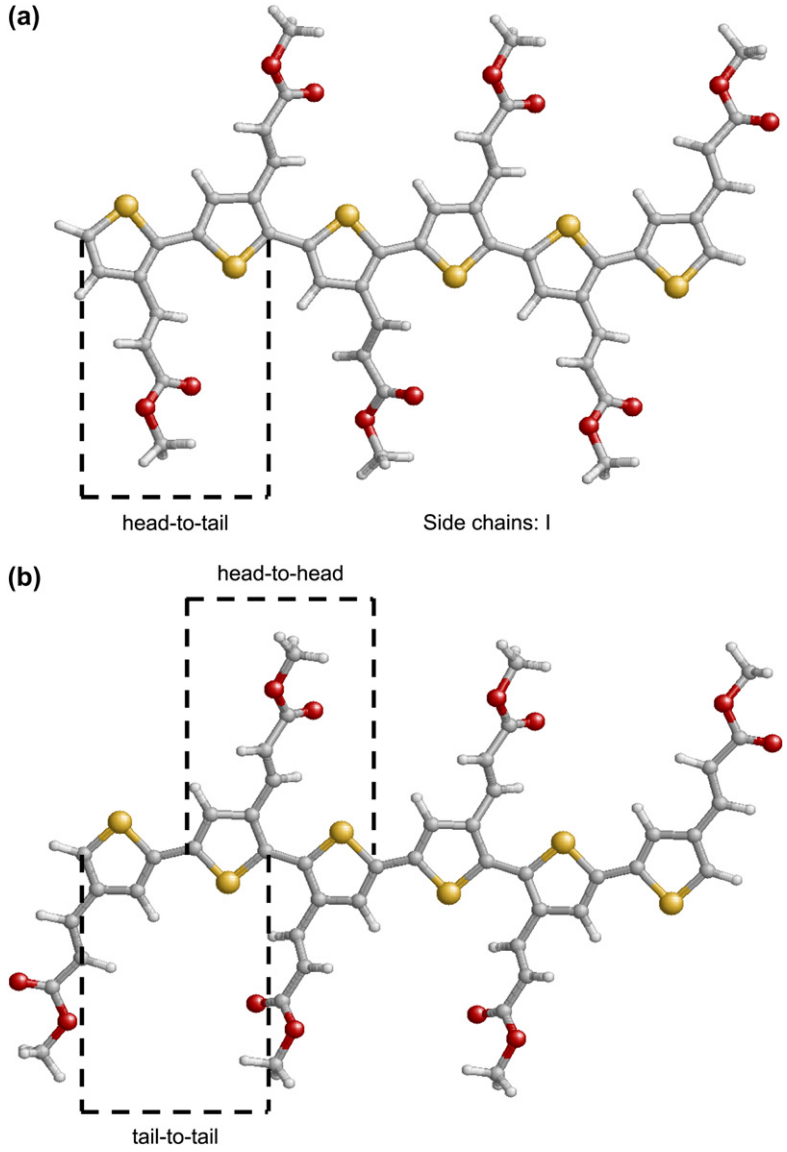

Fig. 4. Models for poly(3-thiophen-3-yl-acrylic acid methyl ester) (PT3AME) constituted by (a) head-to-tail linkages and (b) alternated tail-to-tail and head-to-head linkages. The former model has been proposed for the system under study.

As can be seen, the ε_g of PT3AME was predicted to be 0.38 eV larger than that calculated for polythiophene (1.82 eV) using the same DFT method. Thus, the AME side groups of *n*-T3AME oligomers reduce the energy of the HOMO and LUMO with respect to the corresponding unsubstituted oligothiophenes. However, the stabilization of the former is slightly greater than that of the latter, which increases the ε_g value.

Chemically synthetized PT3AME was soluble in a variety of polar organic solvents such as acetone and DMSO, although it was insoluble in water. The spectral properties were consistent with the structure of the polymer. Fig. 7 compares the FTIR spectrum of PT3AME with that of the monomer 3TA. A detailed analysis of the absorption bands allows us to confirm that the polymer was successfully obtained by chemical oxidative reaction with $FeCl_3$. In Fig. 7a, the aromatic C–H stretch at $\sim$3070 cm^{-1} can be attributed to the β-hydrogen of the thiophene ring, whereas the band at $\sim$3090 cm^{-1} is related with the α-hydrogen position of 3TA. The latter band is not observed in the FTIR spectrum of PT3AME indicating that thiophene rings are linked by the α positions. Furthermore, the very sharp band at 793 cm^{-1}, which is typically associated with the α-C–H out-of-plane deformation, is completely absent in the polymer spectrum (Fig. 7b) confirming the formation of the polymer. On the other hand, the double bond and the carbonyl of the AME side groups are evidenced in the polymer by the $\sim$1630 and 1712 cm^{-1} regions, respectively. More details about the physical and spectroscopic properties of PT3AME will be reported in a near future, together with those of a wide family of polythiophene derivatives soluble in polar solvents [26].

Fig. 8 shows the UV spectra recorded in acetone and DMSO solutions. The first absorption band on the low energy side of the spectra arises from the π–π* transition in the

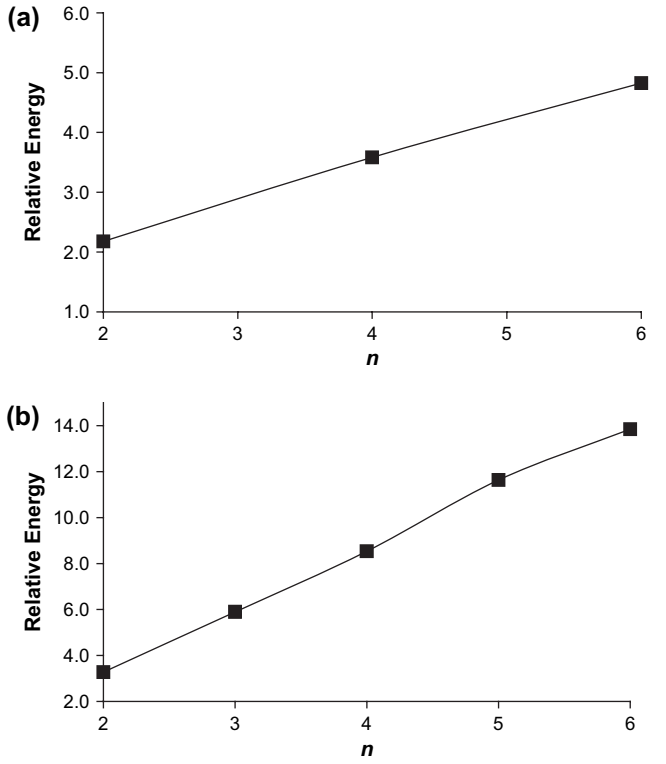

Fig. 5. Variation of the relative energy (in kcal/mol) against n, where n is the number of monomeric units, between (a) the two models constructed for n-T3AME (energies of the model obtained considering alternated tail-to-tail and head-to-head linkages are relative to the most stable one, which was constructed using head-to-tail linkages); and (b) the fully optimized and all-*anti* conformations for the model obtained using head-to-tail linkages. Calculations were performed considering $n = 2$, 4 and 6.

delocalized electron system along the chain. Thus the energy of the band gap of the conduction can be estimated from the intersection of a tangent placed over the inflection point of this curve and the wavelength axes [41,43,44]. The broad absorption band on the blue side of the spectra is the result of a serial of different higher energy intra- and inter-chain electron transitions in the polymer matrix. Interestingly, the high energy region seems to be dominant for PT3AME. This should be attributed to the π electrons in the side chain that either expand the electronic delocalization, *i.e.* the importance of the absorption due to $\pi-\pi^*$ transition in the delocalized electron system along the chain is less pronounced, or cause other electronic states by π-stacking with monomeric units of neighboring chains.

The ε_g values estimated with the tangential through the turning point of the low energy side of the UV–visible spectra in acetone and DMSO are 2.54 and 2.48 eV, respectively. These gaps are only about 0.2 eV larger than that predicted by theoretical calculations. A similar trend was found for unsubstituted polythiophene, where the calculated ε_g (1.82 eV) [22] was 0.2 eV lower than the value determined experimentally (~2.0 eV) [45,46]. The overall results indicate that DFT calculations are able to provide very reliable estimations of the gap, the small underestimation being probably due to the omission of the environment and/or the lack of the structural defects along the polymer chain in the theoretical model.

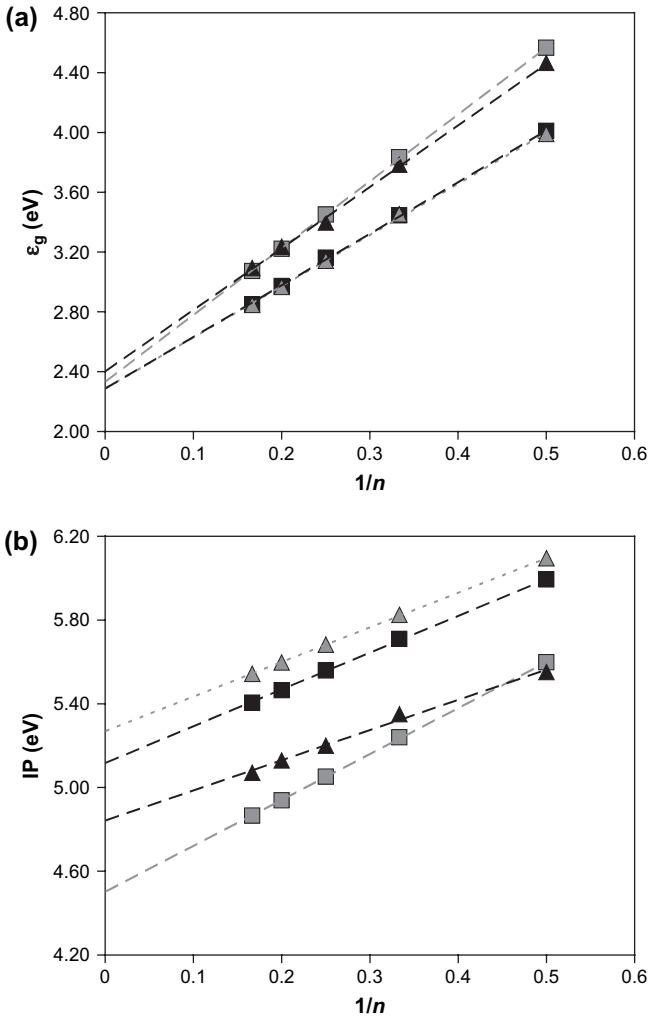

Fig. 6. Variation of (a) ε_g (in eV) and (b) IP (in eV) against $1/n$, where n is the number of monomeric units, for PT3AME (black squares), M-1 (gray triangles), M-2 (black triangles) and M-3 (gray squares). The dashed lines correspond to the linear regressions used to obtain the ε_g for infinite chain systems.

The results provided by UV–visible spectra can be rationalized by comparing the aromaticity of the cycles and the bond length alternation pattern calculated for PT3AME and polythiophene. The Julg parameter, JP, calculated for three cycles going from the edge to the middle of oligomers with

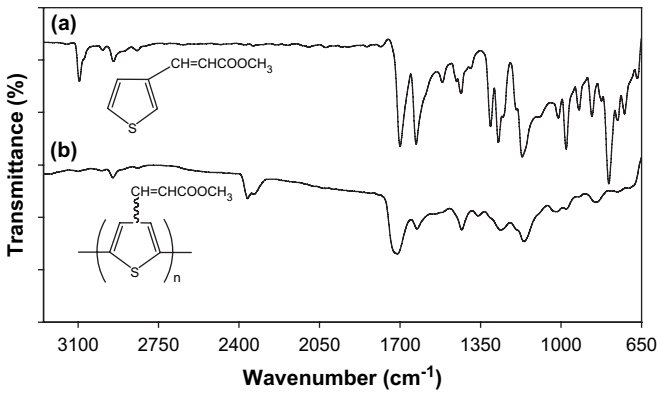

Fig. 7. FTIR spectrum of (a) 3-thiophen-3-yl-acrylic acid (3TA) and (b) poly-(thiophen-3-yl-acrylate acid methyl ester) (PT3AME).

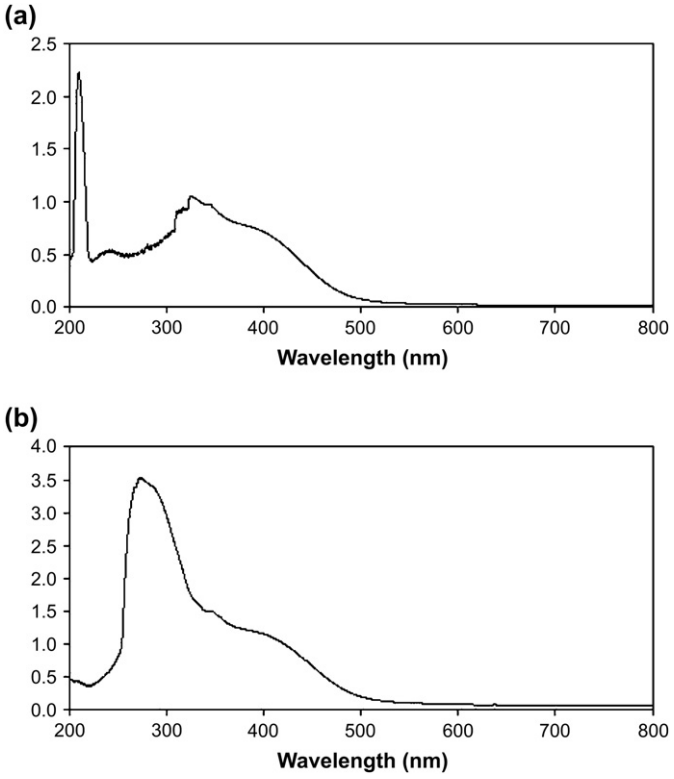

Fig. 8. UV–visible spectrum of poly(3-thiophen-3-yl-acrylic acid methyl ester) (PT3AME) in (a) acetone and (b) DMSO.

$n = 6$, *i.e.*6-T3AME and 6-Thp, respectively, are listed in Table 4, where the inter-ring bond lengths (d_{inter}) are also displayed. The JP provides geometric indication of the delocalization within the diene part of the ring, giving information about the aromaticity in the heterocyclic structure. Note that the π-conjugation along the *cis*-1,3-butadiene unit will be more pronounced when the JP becomes closer to one.

As a general trend for both 6-T3AME and 6-Thp, in the inner rings, which are the most representative, JPs are larger and d_{inter} values are shorter than in the outer rings. Furthermore, JP and d_{inter} values vary with the following sequence 6-T3AME < 6-Thp and 6-T3AME > 6-Thp, respectively, which reflect the decrease of conjugation upon substitution. The bond length alternation patterns displayed in Fig. 9 supports this view. These results indicate that experimental observations discussed above, *i.e.* transitions in the high energy region of the UV–visible spectra of PT3AME and ε_g(PT3AME) > ε_g-(polythiophene) are consequence of the low conjugation of

Table 4
Julg parameters (plain) and inter-ring distance (italic; in Å) calculated for 6-T3AME and 6-Thp[a]

	Cycle 1	Cycle 2	Cycle 3
6-T3AME	0.783–1.463	0.839–1.470	0.842–1.462
6-Thp	0.807–1.461	0.844–1.459	0.849–1.458

[a] Results are displayed for the first three cycles of each oligomer, *i.e.* Cycles 1, 2 and 3. It is worth noting that, when a planar all-*anti* conformation is considered, the remaining cycles are equivalent to these ones due to the molecular symmetry of 6-T3AME and 6-Thp.

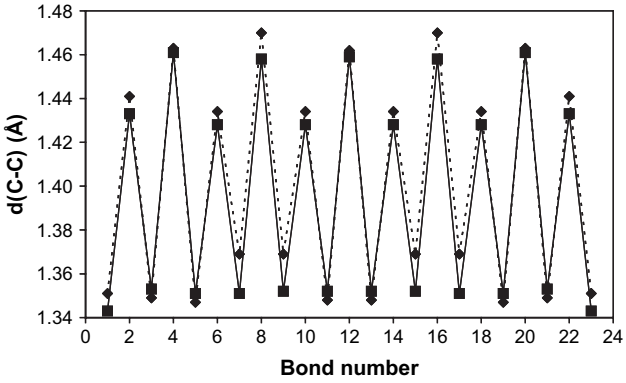

Fig. 9. C–C bond distances along the conjugated π-system of 6-T3AME and 6-Thp.

PT3AME with respect to polythiophene. Thus, the incorporation of the conjugated AME side groups does not improve the electronic delocalization along the polymer chain as was initially assumed.

3.4. Variation of the electronic properties produced by small chemical modifications on the acrylic acid methyl ester substituents

Finally, we have used theoretical calculations to investigate the variation of the gap and IP when small chemical modifications are introduced in the side group of PT3AME. Specifically, we replaced the AME side group (R = –CH=CH–COO–CH_3) in the model proposed in Fig. 4a by R = –CH=CH–COOH (M-1), R = –CH_2–CH_2–COO–CH_3 (M-2) and R = –CH_2–COO–CH_3 (M-3). It should be noted that these predictions are significantly important for future studies, in which we would like to design polythiophene derivatives soluble in a wider set of polar solvents than PT3AME, in particular water.

As the side groups of M-1, M-2 and M-3 are similar in size to that of AME, it is reasonable to assume that the model previously proposed for PT3AME is also valid for these polymers. Molecular geometries of oligomers formed by $n = 2–6$ monomeric units were optimized at the HF/6-31G(d) level for such three systems, while single point calculations at the B3PW91/6-31G(d,p) level were performed on the optimized geometries. Graphical representation of ε_g and IP against $1/n$, which are included in Fig. 6, evidences linear correlations similar to those previously discussed for PT3AME.

The values of ε_g extrapolated for an infinite chain of M-1, M-2 and M-3 were 2.28, 2.32 and 2.35 eV, respectively. These results indicate that substitution of AME by the three groups mentioned above does not produce significant changes in the gap. Specifically, the ε_g calculated for M-1 is identical to that predicted for PT3AME, while the ε_g of M-2 and M-3 are slightly larger, *i.e.* 0.04 and 0.07 eV, respectively. Accordingly, changes in the side chain are expected to improve the solubility of the polymer in polar solvents without altering this electronic property. On the other hand, the IP predicted for M-1, M-2 and M-3 are 5.27, 4.84 and 4.50 eV, respectively.

As can be seen, the ability to be oxidized is higher for the two compounds without double bond in the side group, especially for that with the carboxylate group and the thiophene ring separated by only one methylene unit (M-3).

4. Conclusions

In this work we applied ab initio quantum chemical methods to provide a model for PT3AME. Calculations on 2-T3AME indicated that the isomer with the side groups attached at positions 4,4′ is 1.7 and 3.0 kcal/mol more stable than the isomer substituted at 3,4′ and 3,3′ positions, respectively. Furthermore, the arrangement I was predicted to be the most favored for the AME side groups independent of the isomer. On the basis of these structural results, a model based on head-to-tail linkages was proposed for PT3AME, which was used to evaluate the electronic properties of this polymer through DFT calculations. The ε_g and IP predicted for PT3AME were 2.28 and 5.11 eV, respectively. This gap value is in excellent agreement with ε_g derived from UV–visible experiments. In spite of the conjugated nature of AME groups, the ε_g of PT3AME is larger than that obtained for unsubstituted polythiophene. Thus, analysis of electronic parameters reveals that the delocalized electron system along the chain is less aromatic in PT3AME than in unsubstituted polythiophene, which explains experimental observations. These results have been used to predict how chemical modifications oriented to improve the solubility of PT3AME affect the electronic properties of the polymer.

Acknowledgements

This work has been supported by MCYT and FEDER with grant MAT2006-04029. PP acknowledges the fellowship given by the Generalitat de Catalunya (DURSI). Authors are indebted to the Centre de Supercomputació de Catalunya (CESCA) for computational facilities.

References

[1] Roncali J. Chem Rev 1992;92:711.
[2] Roncali J. Chem Rev 1997;97:173.
[3] Skotheim TA. In: Elsenbaumer RL, Reynolds JR, editors. Handbook of conducting polymers. 2nd ed. New York: Marcel Dekker; 1998.
[4] Garnier F. Angew Chem Int Ed Engl 1989;28:513.
[5] Chen TA, Wu X, Rieke RD. J Am Chem Soc 1995;117:233.
[6] Roncali J, Garreau R, Delabouglise D, Garnier F, Lemaire M. Synth Met 1989;28:C341.
[7] Souto Maior RM, Hinkelman K, Eckert H, Wudl F. Macromolecules 1990;23:1268.
[8] Demanze F, Yassar A, Garnier F. Adv Mater 1995;7:907.
[9] Kim B, Chen L, Gong J, Osada Y. Macromolecules 1999;32:3964.
[10] Rasmussen SC, Pickens JC, Hutchison JE. Macromolecules 1988;31:933.
[11] Pomeranz M, Yang H, Cheng Y. Macromolecules 1995;28:5706.
[12] Kim YG, Samuelson LA, Kumar J, Tripathy SK. J Macromol Sci 2002;A39:1127.
[13] Rasmussen SC, Pickens JC, Hutchison JE. Chem Mater 1998;10:1990.
[14] McCullough RD, Ewbank PC, Loewe RS. J Am Chem Soc 1997; 119:633.
[15] Ewbank PC, Loewe RS, Zhai L, Reddinger J, Sauve G, McCullough R. Tetrahedron 2004;60:11269.
[16] Chayer M, Faïd K, Leclerc M. Chem Mater 1997;9:2902.
[17] Pomerantz M, Cheng Y. Tetrahedron Lett 1999;40:3317.
[18] Pomerantz M. Tetrahedron Lett 2003;44:1563.
[19] Pomerantz M, Amarasekara AS. Synth Met 2003;135:257.
[20] Pomerantz M, Amarasekara AS, Rasika Dias HV. J Org Chem 2002; 67:6931.
[21] Ocampo C, Curcó D, Alemán C, Casanovas J. Synth Met 2006;156: 602.
[22] Casanovas J, Zanuy D, Alemán C. Polymer 2005;46:9452.
[23] Zotti G, Berlin A. Synth Met 1999;105:135.
[24] Lankinen E, Sundholm P, Talonen H, Grano F, Sundholm J. J Electroanal Chem 1999;460:176.
[25] Dock TJJM, de Ruiter B. Synth Met 1996;79:215.
[26] Pfeiffer P. Ph.D. Thesis, in preparation, Universitat Politècnica de Catalunya.
[27] Hariharan PC, Pople JA. Chem Phys Lett 1972;16:217.
[28] Alemán C, Domingo V, Fajarí LI, Julià L, Karpfen A. J Org Chem 1998; 63:1041.
[29] Alemán C, Casanovas J. J Phys Chem A 2004;108:1440.
[30] Alemán C, Julià L. J Phys Chem 1996;100:1524.
[31] Koopmans T. Physica 1934;1:104.
[32] Gatti C, Frigerio G, Benincori T, Brenna E, Sannicolò F, Zotti G, et al. Chem Mater 2000;12:1490.
[33] Alemán C, Armelin E, Iribarren JI, Liesa F, Laso M, Casanovas J. Synth Met 2005;149:151.
[34] Becke AD. J Chem Phys 1993;98:1372.
[35] Perdew JP, Wang Y. Phys Rev B 1992;45:13244.
[36] Frich MJ, Pople JA, Krishnam R, Binkley JS. Chem Phys 1984;80:3264.
[37] Janak JF. Phys Rev B 1978;18:7165.
[38] Levy M, Nagy A. Phys Rev A 1999;59:1687.
[39] Julg A, François P. Theor Chim Acta 1967;8:249.
[40] Yoshino K, Nakao K, Onoda M, Sugimoto R. Solid State Commun 1989;70:609.
[41] Skotheim TA, Reynolds JR. Handbook of conducting polymers. 3rd ed. Boca Raton: CRC Press; 2007.
[42] Ocampo C, Casanovas J, Liesa F, Alemán C. Polymer 2006;47:3257.
[43] Muhlbacher D, Neugebauer H, Cravino A, Sariciftci NS, van Duren JKJ, Dhanabalan A, et al. Mol Cryst Liq Cryst 2002;385:205.
[44] Eckhardt H, Shacklette LW, Jen KY, Elsenbaumer RL. J Chem Phys 1989;91:1303.
[45] Kobayashi M, Chem J, Chung T-C, Moraes F, Heeger AJ, Wudl F. Synth Met 1984;9:77.
[46] Chung T-C, Kaufman JH, Heeger AJ, Wudl F. Phys Rev B 1984;30:702.